Prolonged dexamethasone exposure enhances zebrafish lateral-line regeneration but disrupts mitochondrial homeostasis and hair cell function

Allison L. Saettele[1], Hiu-tung C Wong[2], Katie S Kindt[2], Mark E Warchol[1,3] and Lavinia Sheets*[1,4]

1. Department of Otolaryngology, Washington University School of Medicine, St. Louis, MO, USA
2. Section on Sensory Cell Development and Function, National Institutes on Deafness and Other Communication Disorders, National Institutes of Health, Bethesda, USA
3. Department of Neuroscience, Washington University School of Medicine, St. Louis, MO, USA
4. Department of Developmental Biology, Washington University School of Medicine, St. Louis, MO, USA

*** Corresponding author**
Lavinia Sheets: sheetsl@wustl.edu

ORCID ID
HTC Wong : 0000-0001-5826-8526
KS Kindt: 0000-0002-1065-8215
ME Warchol: 0000-0002-0445-6318
L Sheets: 0000-0001-5231-2450

Keywords: neuromast, regeneration, dexamethasone, mitochondrial homeostasis

Abstract

The synthetic glucocorticoid dexamethasone is commonly used to treat inner ear disorders. Previous work in larval zebrafish has shown that dexamethasone treatment enhances hair cell regeneration, yet dexamethasone has also been shown to inhibit regeneration of peripheral nerves after lesion. We therefore used the zebrafish model to determine the impact of dexamethasone treatment on lateral-line hair cells and primary afferents. To explore dexamethasone in the context of regeneration, we used copper sulfate ($CuSO_4$) to induce hair cell loss and retraction of nerve terminals, and then allowed animals to recover in dexamethasone for 48 hours. Consistent with previously work, we observed significantly more regenerated hair cells in dexamethasone-treated larvae. Importantly, we found that the afferent processes beneath neuromasts also regenerated in the presence of dexamethasone and formed an appropriate number of synapses, indicating that innervation of hair cells was not inhibited by dexamethasone. In addition to regeneration, we also explored the effects of prolonged dexamethasone exposure on lateral-line homeostasis and function. Following dexamethasone treatment, we observed more negatively charged mitochondrial membrane potentials ($\Delta\Psi m$) in neuromast hair cells and supporting cells. Hair cells exposed to dexamethasone were also more vulnerable to neomycin-induced cell death. In response to a

fluid-jet delivered saturating stimulus, calcium influx through hair cell mechanotransduction channels was significantly reduced, yet presynaptic calcium influx was unchanged. Cumulatively, these observations indicate that dexamethasone enhances hair cell regeneration in lateral-line neuromasts, yet also disrupts mitochondrial homeostasis, making hair cells more vulnerable to ototoxic insults and possibly impacting hair cell function.

Introduction

Glucocorticoids are the major hormones of the stress response pathway. Through interactions with ubiquitously expressed receptors, glucocorticoids are involved in regulating many physiological processes, including circadian cycle, tissue homeostasis, metabolism, and inflammation (Vettorazzi et al., 2021). Synthetic glucocorticoids, such as dexamethasone, are commonly used to treat inner ear disorders, such as sudden hearing loss and Menier's disease, and have been proposed as an intervention to protect against cisplatin ototoxicity (Waissbluth et al., 2013). Achieving therapeutic levels of synthetic glucocorticoids in the inner ear with systemic oral delivery of the drug requires high-dose therapy associated with adverse side effects (Egli Gallo et al., 2013). Furthermore, systemic delivery of glucocorticoids to prevent cisplatin ototoxicity may render some types of malignant cells insensitive to cisplatin chemotherapy (Ge et al., 2012). Consequently, local intratympanic delivery directly into the ear has been tested as a potential method for the prevention and treatment of inner ear disease (Marshak et al., 2014; Patel, 2017). One limitation to this approach is that dexamethasone is rapidly cleared from the middle ear (Salt et al., 2011). Thus, strategies to provide sustained delivery of dexamethasone to the inner ear are an active area of research (Fernandez et al., 2016; Liao et al., 2021). While retention of synthetic glucocorticoids in the ear may provide greater therapeutic benefits, the effects of prolonged dexamethasone exposure on hair cell organ homeostasis and function are not well defined.

The zebrafish model has been used in numerous studies evaluating the effects of dexamethasone exposure on biological processes, including wound repair and complex tissue regeneration. In a previous study, dexamethasone was identified in a large-scale screen as an enhancer of hair cell regeneration after neomycin damage to zebrafish lateral-line organs, as well as inducing addition of hair cells to lateral-line neuromasts in the absence of damage (Namdaran et al., 2012). By contrast, treatment with dexamethasone has been shown to inhibit peripheral nerve and spinal motor nerve regeneration in zebrafish (Bremer et al., 2017; Ohnmacht et al., 2016). Cumulatively, these data suggest that, while dexamethasone potentiates the generation of lateral-line hair cells, reinnervation of dexamethasone-induced hair cells may be impaired.

68 In this study we sought to address two questions: 1) does dexamethasone treatment
69 enhance or inhibit afferent innervation and synapse formation in regenerating lateral-line
70 organs, and 2) does prolonged dexamethasone exposure affect hair cell homeostasis and
71 function? Our results reveal that dexamethasone treatment does not inhibit either afferent
72 innervation or synapse formation in newly produced hair cells. However, dexamethasone
73 treatment does increase mitochondrial activity in existing hair cells and reduces their evoked
74 mechanosensory responses, suggesting that prolonged dexamethasone exposure may
75 adversely affect hair cell function.

76 Materials and Methods

77 *Ethics statement*

78 Experimental procedures were performed with approval from the Washington University
79 School of Medicine or NIH Institutional Animal Care and Use Committee, and in accordance
80 with NIH guidelines for use of zebrafish.

81 *Zebrafish*

82 Adult zebrafish were raised under standard conditions at 27-29°C in the Washington
83 University or NIH Zebrafish Facility. Embryos were raised in incubators at 28°C in embryo
84 media (EM; 15 mM NaCl, 0.5 mM KCl, 1 mM $CaCl_2$, 1 mM $MgSO_4$, 0.15 mM KH_2PO_4, 0.042 mM
85 Na_2HPO_4, 0.714 mM $NaHCO_3$) with a 14 h:10 h light:dark cycle. At 3-4 days post fertilization
86 (dpf), larvae were anesthetized in 0.02% tricaine methanesulfonate (MS-222) and screened for
87 transgenic fluorophores using a Leica MZ10 F stereomicroscope with fluorescence equipped
88 with a GFP and a DSR filter set. After 4 dpf, larvae were raised in 100-200 ml EM media in 250-
89 ml plastic beakers and fed rotifers daily. Sex of the animal was not considered for this study
90 because sex cannot be determined in larval zebrafish.

91 *Transgenic lines*

92 The following transgenic lines were used in this study: *TgBAC(neurod1:EGFP)*
93 (Obholzer et al., 2008); *Tg(myo6b:GCaMP3)* and *Tg(myo6b:mitoGCaMP3)* (Esterberg et al.,
94 2013), *Tg(mpeg1:yfp)* (Roca & Ramakrishnan, 2013), *Tg(tnks1bp1:EGFP)* (Behra et al., 2012)
95 and *Tg(myo6b:GCaMP6sCAAX)* (Sheets et al., 2017).

96 *Copper ablation of neuromasts and dexamethasone post-treatment*

97 To ablate lateral-line neuromast hair cells and induce afferent neurite retraction, 5 dpf
98 larvae were exposed to 3 μM $CuSO_4$ (Sigma-Aldrich, Cat# 451677) diluted in EM in cell
99 strainers (Corning; Cat# 431752) for 1 hour. After exposure, larvae were rinsed, and then

allowed to swim freely during a 2-hour recovery in EM. Immediately following this 2-hour recovery, larvae were moved to 6-well plates (Falcon, Cat# 351146) containing 4 mL EM per well with either 0.1% DMSO (drug carrier alone) or 0.1% DMSO + 10 μM dexamethasone (Sigma-Aldrich, Cat# D1756) for 48 hours. Larvae were maintained at 28°C throughout $CuSO_4$ exposure and dexamethasone post-treatments.

Neomycin ablation of neuromasts with dexamethasone pre-treatment

At 5 dpf, larvae were pre-treated with 0.1% DMSO or 1-50 μM dexamethasone in EM for 24 hours (Fig. 5) or 10 μM for 48 hours (Fig. 9). Following pre-treatment, larvae were rinsed twice and placed in cell strainers, and then exposed to 0-100 μM neomycin (Sigma-Aldrich, Cat# N1876) for 30 minutes. Following neomycin exposure, fish were rinsed and moved to 6-well plates with 4 mL of EM to recover for 1 hour.

Whole-mount Immunohistochemistry

Free-swimming larvae were exposed to DAPI (1:2000, 4 minutes; D3571, Thermo Fisher) to label hair cell nuclei, then sedated on ice for 4 min. For GFP immunolabeling to label the afferent process or for Otoferlin immunolabeling to label hair cells, larvae were fixed (4% paraformaldehyde, 4% sucrose, 150 μM $CaCl_2$, 0.1 M phosphate buffer) in 2 mL Eppendorf tubes overnight at 4-8°C. For synaptic labeling, larvae were fixed for 5 hours at 4-8°C.

Larvae fixed overnight were blocked in phosphate-buffered saline (PBS: 8 g NaCl, 0.2 g KCl, 0.24 g KH_2PO_4, 14.4 g Na_2HPO_4 per 1 L distilled H_2O) with 5% normal horse serum (NHS; Sigma-Aldrich, Cat# H0146), 1% DMSO, 1% Triton X-100 (Sigma-Aldrich, Cat# T8787) for 2 hours at room temperature. Primary antibody exposure was performed in PBS with 2% NHS, 0.1% Triton-X100. Secondary antibody exposure was performed in PBS with 2% NHS. Following all antibody exposures, larvae were rinsed several times in PBS with 0.1% Tween-20 (Sigma-Aldrich, Cat# P9416).

For synaptic labeling, larvae were fixed for 5 hours, permeabilized in ice-cold acetone (-20°C, 5 min, Sigma-Aldrich, Cat# 179124), then blocked in PBS with 2% goat serum (Sigma-Aldrich, Cat# G9023), 1% bovine serum albumin (BSA; Sigma-Aldrich, Cat# A9647), and 1% DMSO for 2 hours. Primary and secondary antibody solutions and all post-antibody rinses were performed in the same PBS, BSA, and DMSO concentration mix used for blocking.

Primary antibodies:

- Mouse IgG2a α-CtBP (1:2000; Santa Cruz Biotech, Inc; Cat#: sc-55502)
- Mouse IgG1 α-MAGUK (K28/86; 1:500; NeuroMab, UC Davis; Cat# 75-029)
- Chicken α-GFP (1:500; Aves Labs, Inc; Cat# GFP-1020)

133 - Mouse IgG2a α-Otoferlin (1:500; Developmental Studies Hybridoma Bank; HCS-
134 1)

135 Secondary antibodies:

136 - Goat α-chicken (Alexa 488) - neurites
137 - Goat α-mouse IgG1 (Alexa 488) – MAGUK
138 - Goat α-mouse IgG1 (Alexa 647) - MAGUK
139 - Goat α-mouse IgG2a (Alexa 647) - CtBP
140 - Goat α-mouse IgG2a (DyLight 550/Alexa546) – CtBP

141 All fish were rinsed in PBS prior to being mounted on glass slides in elvanol (13% w/v
142 polyvinyl alcohol, 33% w/v glycerol, 1% w/v DABCO (1,4 diazobicylo[2,2,2] octane) in 0.2 M
143 Tris, pH 8.5) and #1.5 cover slips.

144 *FM1-43 labeling:*

145 Larvae were anesthetized in EM containing 0.01% Tricaine (EMT), exposed to 3 μM
146 FM1-43 (N-(3-triethylammoniumpropyl)-4-(4-(dibutylamino)-styryl) pyridinium dibromide;
147 ThermoFisher, Cat# T3163) for 20 seconds, rinsed in EMT, and then mounted on a FluoroDish
148 (World Precision Instruments, Inc., Cat# FD3510) in low-melt agarose (Invitrogen, Cat# 16520)
149 containing 0.01% Tricaine (LMAT). The agarose was allowed 2.5 minutes to solidify before
150 covering in EMT and imaging.

151 *TMRE labeling*

152 Larvae were exposed to 250 nM tetramethylrhodamine ethyl ester perchlorate (TMRE,
153 Thermo Fisher, Cat# T669) diluted in EM for 25 minutes while wrapped in foil, then rinsed,
154 allowed to equilibrate for 10-15 minutes, and mounted on a FluoroDish in LMAT. The agarose
155 was allowed 2.5 minutes to solidify before covering in EMT and imaging.

156 *Confocal imaging*

157 Most confocal images were acquired via an ORCA-Flash 4.0 V3 camera (Hamamatsu)
158 using a Leica DM6 Fixed Stage microscope with an X-Light V2TP spinning disc confocal (60
159 micron pinholes) equipped with an LDI-7 laser diode illuminator (89 North). Image acquisition
160 was controlled by MetaMorph software. *For fixed imaging:* z-stack images ~10-15 μm depth with
161 a z-step of 0.2 μm were acquired using a 63x/1.4 N.A. oil immersion objective. *For live imaging:*
162 larvae were anesthetized with 0.01% tricaine in EM, then mounted lateral-side up on a thin layer
163 of 1% low-melt agarose in a tissue culture dish with a cover-glass bottom (FluoroDish; World
164 Precision Instruments) and covered in EMT media. Z-stack images of neuromast L3-5 were
165 acquired with a 63x/0.9 N.A. water immersion objective. Z- acquisition parameters with X-light

166 spinning disc: z step of 1 μm, laser "20% power" for all wavelengths, 100 ms per frame for fixed
167 imaging, 120 ms per frame for live imaging. Images in Fig. 5 were acquired using an LSM 700
168 laser scanning confocal microscope with a 63x 1.4 NA Plan-Apochromat oil-immersion objective
169 (Carl Zeiss). Confocal z-stacks of ~15 μm depth were acquired with a z-step of 1 μm.

170 *Confocal image processing and analysis*

171 Fiji (ImageJ software) was used to process and analyze most confocal images
172 (Schneider et al., 2012). To analyze macrophage activation and inflammation, confocal images
173 were reconstructed and analyzed using Volocity software (Quorum Technologies). Subsequent
174 image processing for display within figures was performed using Illustrator software (Adobe).

175 Hair cell counts were quantified from hair cell specific DAPI labeled nuclei or from cells
176 immunolabeled for Otoferlin (HCS-1; Fig. 5). To quantify hair cell synapses, raw images
177 containing single immunolabel were converted to 8-bit, then subtracted for background using a
178 20-pixel (CtBP) or 10-pixel (MAGUK) rolling ball radius. Puncta were defined as regions of
179 immunolabel with pixel intensity above a determined threshold: threshold for Ribeye label was
180 calculated using the Isodata algorithm and threshold for MAGUK label was calculated using the
181 Yen algorithm. Intact synapses were defined as CtBP immunolabel juxtaposed with MAGUK
182 and quantified by scrolling through image z-stacks.

183 To measure neurite length, the ImageJ plugin Simple Neurite Tracer (Longair et al.,
184 2011) was used on z-stack images of GFP-labeled afferent neurons. Following ImageJ's Basic
185 Instructions, which can be found in the Help drop-down menu of the Tracer plugin, neurites
186 were traced by scrolling through the z-stack and creating paths. All neurite structures making up
187 the basket-like processes that surround the neuromast were included in the paths, as well as
188 the stalk at the base of the neuromast where innervating neurites emerged from the main
189 afferent neuronal tract and any meandering projections coming off the dendritic basket. The
190 Simple Neurite Tracer automatically detected the path set between two designated points and
191 calculated a measured length in microns. Any branches emerging from and between paths were
192 measured as separate paths. Once fully traced, all paths within the dendritic basket were then
193 added together to get the total neurite length within the neuromast.

194 Macrophage density was quantified by scrolling through image z-stacks and counting the
195 number of macrophages within 25 μm radius of a neuromast (using a circle inscribed on the
196 neuromast). The number of macrophages contacting a neuromast was determined by scrolling
197 through the x-y planes of each image stack (1 μm interval between x-y planes, 15 μm total
198 depth) and counting macrophages that were in direct contact with Otoferlin-labeled hair cells.
199 Finally, the number of macrophages that had internalized Otoferlin-immunolabeled material (hair

200 cell debris) was counted and assumed to reflect the number of phagocytic events. For each
201 metric, the recorded number reflected the activity of a single macrophage, i.e., a macrophage
202 that made contacts with multiple hair cells and/or had internalized debris from several hair cells
203 was still classified as a single 'event.'

204 To measure the baseline fluorescence intensity of indicators across whole neuromasts,
205 images containing single channels were background-subtracted using a rolling ball radius of the
206 following sizes: images containing cytoGCaMp3 or mitoGCaMP3 (50-pixel), images containing
207 FM1-43FX or TMRE label (100-pixel). Whole neuromasts were delineated based on hair cell
208 specific DAPI label in maximum-intensity projections, and mean intensity of the indicator was
209 measured. Measurements from each experimental trial were normalized to the control median
210 value. To accommodate nested data and ensure statistical rigor, we preformed subsequent
211 statistical analysis on average value of measurements from multiple neuromasts (L3, L4, L5)
212 within an individual fish, such that each fish provided a single data point.

213 *Functional calcium imaging*

214 GCaMP6s-based calcium imaging was used to examine evoked signals in zebrafish hair
215 bundles and presynapses, as described previously (Lukasz & Kindt, 2018). Briefly, after 48-hour
216 dexamethasone treatment, individual 7 dpf larvae were first anesthetized with EMT. Pins were
217 used to restrain larvae onto a Sylgard-filled recording chamber. To suppress the movement,
218 alpha-bungarotoxin (125 μM, Tocris) was injected into the cavity of the heart. Larvae were then
219 immersed in extracellular imaging solution (in mM: 140 NaCl, 2 KCl, 2 $CaCl_2$, 1 $MgCl_2$ and 10
220 HEPES, pH 7.3, OSM 310 +/- 10) without tricaine. A fluid jet was used to mechanically stimulate
221 hair bundles (L1-L4) with posterior fluid-flow for 500 ms.

222 To detect evoked calcium responses, images were acquired using a Bruker Swept-field
223 confocal microscope (Bruker Inc), with a Nikon CFI Fluor 60x 1.0 NA water-immersion objective.
224 A Rolera EM-C2 CCD camera (QImaging) was used to detect signals. To measure
225 GCaMP6sCAAX signals, images were acquired with 2x2 binning using a 35 μm slit at 10 Hz in
226 z-stacks of 5 planes every 2 μm or 0.5 μm for presynaptic and hair bundle measurements. High
227 speed imaging along the z-axis was accomplished by using a piezoelectric motor (PICMA P-
228 882.11–888.11 series, Physik Instrumente GmbH). Sequential evoked GCaMP6sCAAX
229 acquisitions were separated by at least 5 min.

230 To quantify the magnitude of evoked GCaMP6s signals, images were processed in FIJI.
231 Z-stacks were max-projected, and images at each timepoint were aligned using StackReg
232 (Thevenaz et al., 1998). A 5 μm and 1.31 μm diameter circular ROI was drawn over each hair
233 cell base and hair bundle respectively to make intensity measurements. To plot evoked changes

234 in GCaMP6s intensity, the baseline (F_0, signal during the 2 s pre-stimulus period) was used to
235 plot the relative change in fluorescent signal from baseline ($\Delta F/F_0$). The magnitude of evoked
236 calcium signals was determined using $\Delta F/F_0$ plots. The baseline GCaMP6s signal F_0 was used
237 to estimate the resting calcium levels in each hair bundle or presynaptic region. The response
238 magnitudes or resting GCaMP6s levels for each neuromast were averaged to obtain a single
239 point per neuromast.

240 *Statistical analysis*

241 Statistical analyses were performed using Prism 9 (Graphpad Software Inc). Datasets
242 were confirmed for normality using the D'Agostino-Pearson test when appropriate. Statistical
243 significance between two groups was determined by an unpaired Student's t-test or an unpaired
244 Welch's unequal variance t-test, depending on the normality of the dataset. Statistical
245 significance between multiple groups with normal distributions was determined by one-way
246 ANOVA and appropriate post-hoc tests, and statistical significance between multiple groups
247 with non-normal distributions was determined by a Kruskal-Wallis test and appropriate post-hoc
248 tests. For datasets dependent on multiple independent variables, statistical significance was
249 determined using two-way ANOVA and appropriate post-hoc tests.

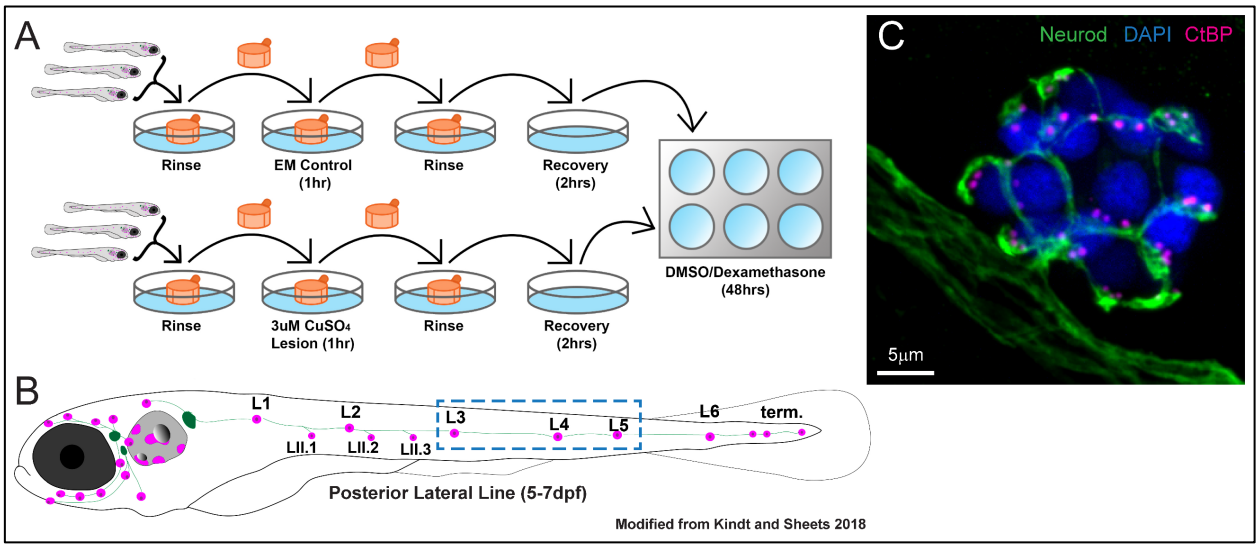

Figure 1. Workflow of $CuSO_4$ lateral-line lesion and dexamethasone exposure
(A) Diagram of workflow for CuSO4 lesions and dexamethasone exposure. Larvae (5 dpf) were placed into cell strainers and moved between rinse and lesion steps, while being allowed to swim freely during recovery and dexamethasone exposure. (B) Diagram of a 5-7dpf zebrafish larvae showing the distribution of lateral line neuromasts (magenta) and innervating afferent nerves (green). This study focused on neuromasts L3, L4, and L5 (blue dashed-line box). (C) Representative maximum intensity projection of confocal z-stack image of neuromast L4 in a 7 dpf zebrafish larvae. Labels: afferent neurons labeled with GFP (green; tgBAC(neurod1:GFP), DAPI-labeled hair-cell nuclei (blue), and immunolabeled presynaptic ribbons (magenta; pan-CtBP).

250 Results

251 **Dexamethasone enhances regeneration and reinnervation of neuromast hair cells**
252 **following $CuSO_4$ lesion.**

253 In two separate small molecule screens using zebrafish larvae, dexamethasone has
254 been identified as an enhancer of hair cell regeneration in lateral-line neuromasts and an
255 inhibitor of peripheral fin nerve regeneration (Bremer et al., 2017; Namdaran et al., 2012).
256 Dexamethasone has also been reported to enhance axon regeneration in rats, following injury
257 (Feng & Yuan, 2015). We therefore addressed whether dexamethasone influences afferent
258 reinnervation and hair cell synapse regeneration in zebrafish lateral-line neuromasts. To induce
259 injury, we exposed animals to copper sulfate ($CuSO_4$), which induces loss of lateral-line hair
260 cells and considerable retraction of afferent nerve terminals (Hardy et al., 2021; Mackenzie &
261 Raible, 2012; Olivari et al., 2008). Five-day old zebrafish larvae were treated in either 3 μM
262 $CuSO_4$ in embryo media (EM) or EM alone for 1 hour. After $CuSO_4$ exposure, the animals were
263 allowed to recover for 2 hours, and then transferred to EM containing either 10 μM
264 dexamethasone or drug carrier alone (0.1% DMSO) for 48 hours (Fig. 1A). After 48 hours we
265 assessed the extent of afferent reinnervation and hair cell and synapse regeneration. We

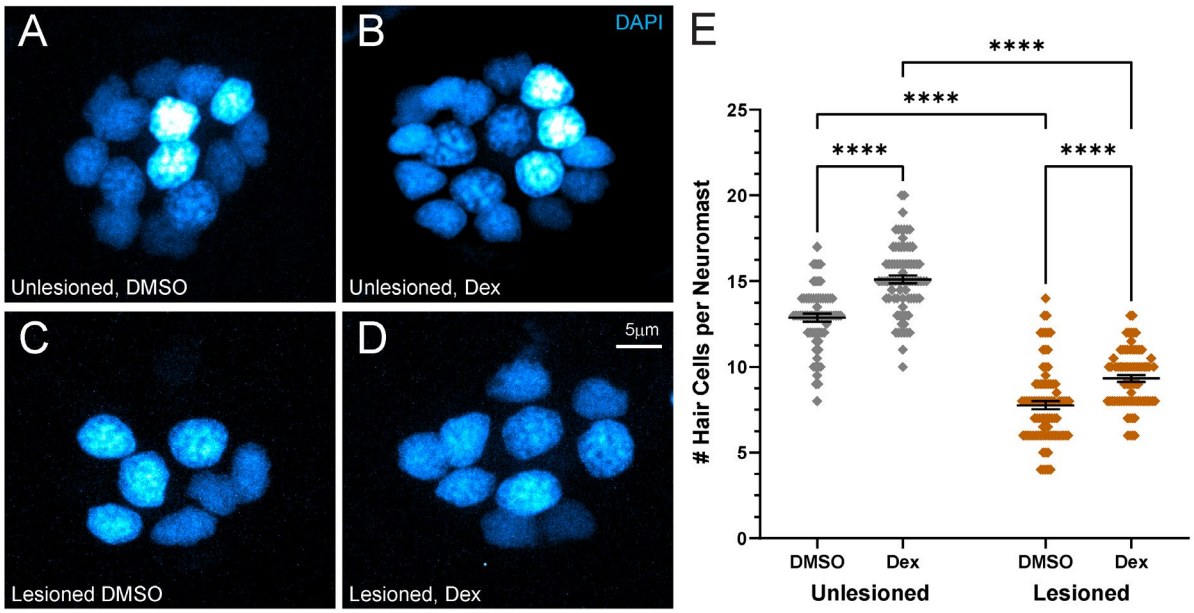

Figure 2. Dexamethasone increased hair cell number in intact and regenerating neuromasts
(A-D) Representative maximum intensity projection images of 7dpf neuromasts, with DAPI-labeled hair cell nuclei (blue). Larval lateral line neuromasts were either left intact (unlesioned) (A, B) or lesioned by treatment with 3μM $CuSO_4$ for 1 hour (C, D). Larvae were then allowed to recover for 2hrs, then exposed for 48 hr to either 0.1% DMSO (carrier) (A, C) or dexamethasone (B, D). (E) Scatter plot graph of hair cell number per neuromast. Bars indicate mean and SEM. Each dot represents a single neuromast. Both intact (unlesioned) and regenerating neuromasts showed a significant increase in the number of hair cells per neuromast in dexamethasone-treated fish relative to DMSO controls (****adjusted $P<0.0001$). N= 5-10 fish per condition per trial; 7 experimental trials.

266 focused on posterior lateral-line neuromasts L3-L5 for analysis (Fig. 1B). To examine afferent
267 reinnervation and hair cell regeneration we visualized afferent nerve fibers labeled with GFP as
268 well as hair cell nuclei labeled with DAPI (Fig. 1C). In agreement with previous observations of
269 lateral-line organs injured with neomycin, we observed a significantly greater number of
270 regenerated hair cells per neuromast in larvae exposed to dexamethasone during regeneration
271 compared to controls (Fig. 2 C-E; orange points). Additionally, among fish that were not
272 exposed to $CuSO_4$ (unlesioned), significantly more hair cells per neuromast were observed in
273 fish that were exposed to dexamethasone (Fig. 2 A,B,E; gray points). This observed increase in
274 hair cell number per neuromast has been previously shown to be due to increased proliferation
275 of hair cell precursors rather than prevention of hair cell turnover (Namdaran et al., 2012). These
276 results therefore confirm that dexamethasone enhances hair cell regeneration and stimulates
277 hair cell precursors to divide, even in the absence of injury.

278 To determine whether dexamethasone treatment enhanced or inhibited afferent
279 innervation of hair cells, we measured the length of innervating afferent processes in both
280 unlesioned and lesioned neuromast after regeneration (Fig. 3 A-D). In neuromasts that had
281 regenerated after $CuSO_4$-induced lesions, we observed that the average length of afferent
282 processes per neuromast was significantly greater in animals that recovered in dexamethasone
283 compared to animals exposed to drug carrier alone (Fig 3 C-E (orange box plots); ****adjusted
284 $P<0.0001$). We reasoned that increased neurite length in dexamethasone-treated animals was
285 related to the greater number of regenerated hair cells per neuromast. To verify this idea,
286 neurite length was normalized relative to the number of hair cells in each neuromast. Following
287 normalization, we observed no difference in relative neurite length per hair cell in animals
288 recovered in dexamethasone vs. those in drug carrier alone (Fig 3F (orange box plots); adjusted
289 $P=0.5630$). In unlesioned animals treated with dexamethasone, we observed no change in
290 afferent neurite length per neuromast (Fig. 3 A,B,E (gray box plots); adjusted $P=0.8215$) and a
291 modest reduction the relative neurite length per hair cell that was not statistically significant (Fig
292 3F (gray box plots); adjusted $P=0.2959$). These data indicate that dexamethasone treatment
293 enhanced the formation of afferent processes in regenerating neuromasts, perhaps to
294 accommodate a greater number of regenerated hair cells. By contrast, in unlesioned
295 neuromasts dexamethasone did not promote the addition of afferent neurites to accommodate
296 additional hair cells.

297 In addition to quantifying hair cell numbers and neurite length, we also quantified the
298 number of intact synapses per hair cell (Fig. 4 A-D; defined as presynaptic ribbons adjacent to

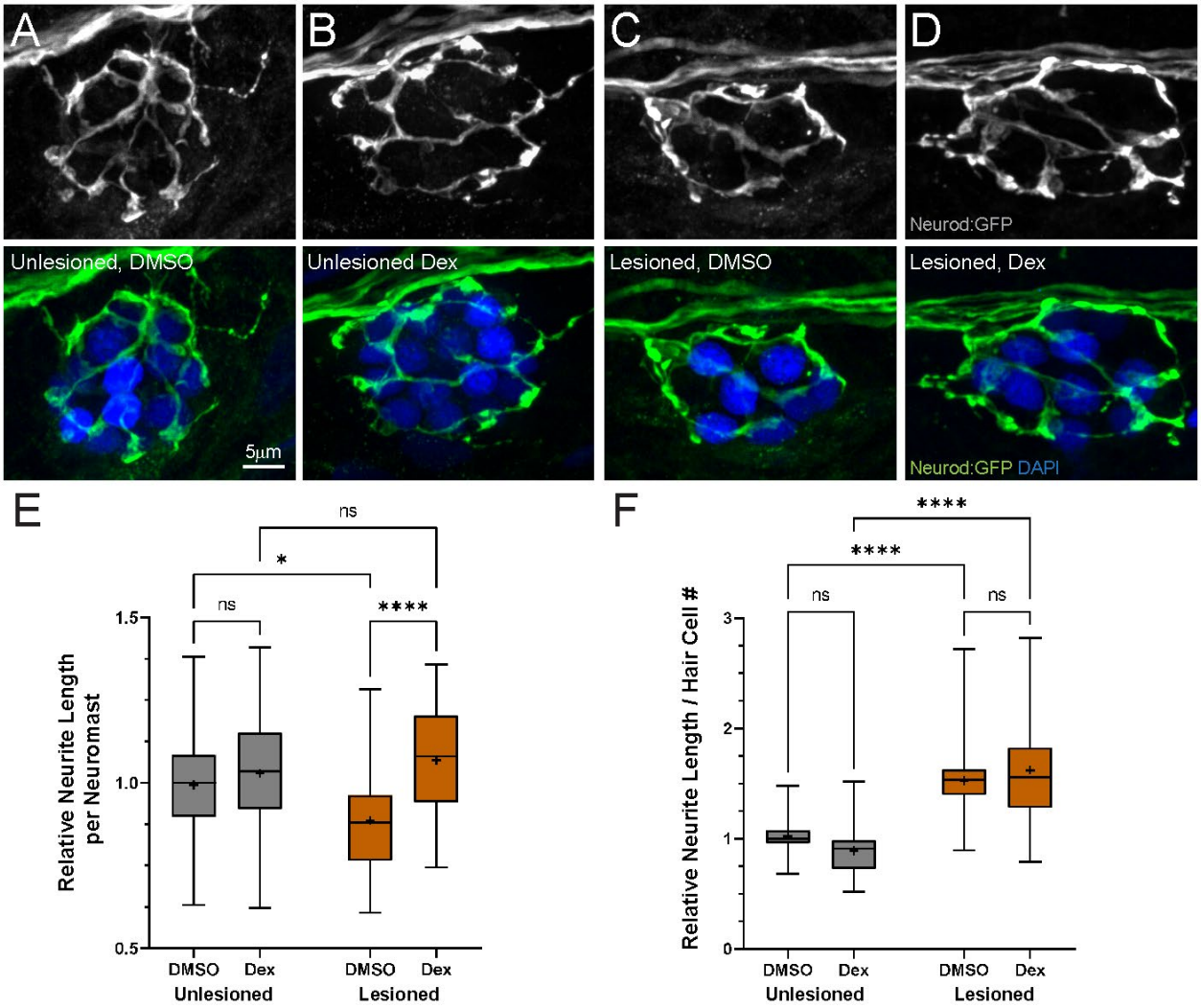

Figure 3. Dexamethasone enhanced afferent innervation of regenerating neuromasts
(A-D) Representative maximum intensity projection images of pLL neuromasts in 7dpf tgBAC(neurod1:GFP) larvae showing afferent neurons (green) and DAPI-labeled hair-cell nuclei (blue). Neuromasts were either unlesioned (A, B) or lesioned with $CuSO_4$ (C, D), then allowed to regenerate for 48 hr while exposed to DMSO (carrier) (A, C) or dexamethasone (B, D). (E-F) Box plots of neurite length per neuromast (E) and neurite length per hair cell (F), with whiskers at min/max and mean values marked with "+". Data for each experimental trial were normalized to the median value of unlesioned controls. Regenerating neuromasts (orange plots) in dexamethasone-treated fish had significantly longer neurites per neuromast (E) (****adjusted P<0.0001), however the difference in length in dexamethasone-treated fish was not significant relative to the total number of hair cells/neuromast, when compared to DMSO controls (F). N=4-7 fish per condition per trial; 6 experimental trials.

postsynaptic densities). We observed no difference in synapse counts between dexamethasone-treated and 0.1% DMSO controls when comparing unlesioned neuromasts or when comparing $CuSO_4$ lesioned neuromasts following regeneration (Fig. 4 E). Notably, we did observe significantly more intact synapses per hair cell in all regenerating neuromasts relative to unlesioned neuromasts (Fig 4 E; adjusted ***P=0.0003 (DMSO), * P=0.0202 (Dex)). Similar observations have been reported in regenerating neuromast hair cells (Hardy et al., 2021; Suli

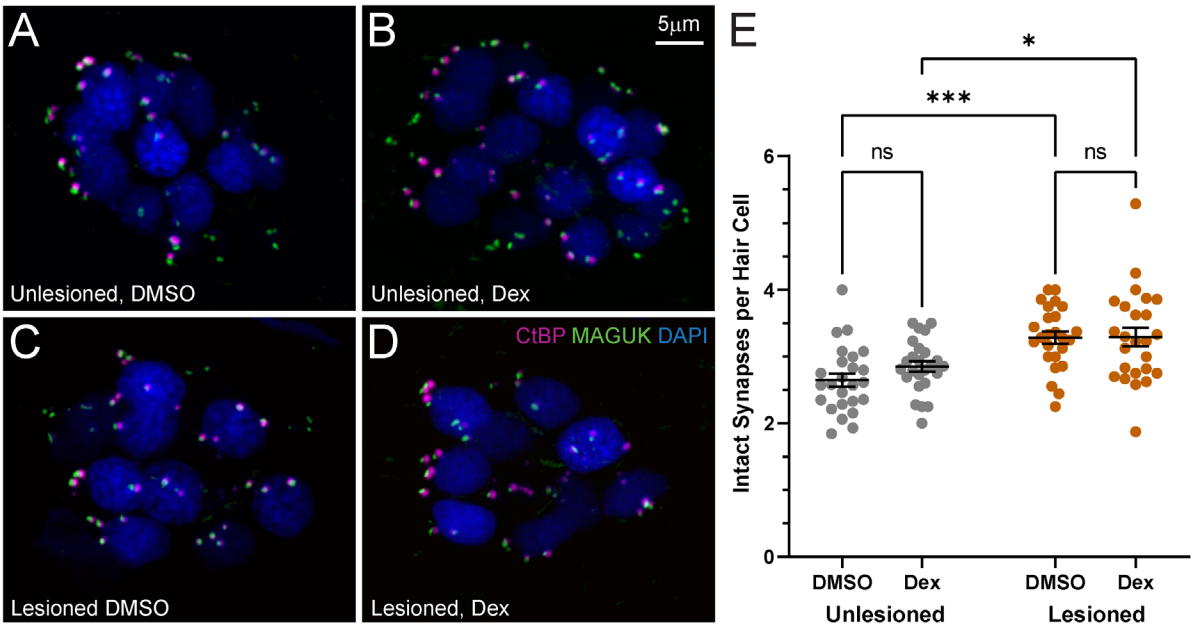

Figure 4. Dexamethasone exposure did not affect afferent synapse number in neuromast hair cells
(A-D) Representative maximum intensity projection images of 7dpf pLL neuromasts, with hair cell presynaptic ribbons labeled via CtBP antibody (magenta), post-synaptic densities labeled via MAGUK antibody (green), and hair cell nuclei labeled with DAPI (blue). Neuromasts were either unlesioned (A, B) or lesioned with $CuSO_4$ (C, D), then allowed to regenerate for 48 hr while exposed to DMSO (carrier) (A, C) or dexamethasone (B, D). (E) Scatter plots with mean and SEM bars showing no significant difference in the number of intact synapses in dexamethasone-treated fish, compared to DMSO controls for both lesioned and intact neuromasts. Notably, a significantly greater number of intact synapses per hair cell were observed in regenerating neuromasts relative to neuromasts that were not lesioned (adjusted ***P=0.0003 (DMSO), * P=0.0202 (Dex)). N=5 fish per condition per trial; 4 experimental trials.

et al., 2016) and may reflect ongoing synaptic refinement akin to that observed in developing cochlear hair cells (Michanski et al., 2019). Overall, these results suggest that dexamethasone treatment enhances afferent neurite outgrowth in regenerating neuromasts and does not impact synapse formation in newly formed hair cells in regenerating or unlesioned neuromasts.

Pretreatment with dexamethasone does not inhibit macrophage response to hair cell injury

Dexamethasone inhibits inflammation and macrophage activation, and various studies indicate dexamethasone's anti-inflammatory action can influence nerve regeneration (Valledor & Ricote, 2004). Previous work has shown that macrophages are recruited to lateral-line organs after injury induced by the ototoxin neomycin (Warchol et al., 2021). We therefore assessed whether dexamethasone inhibited macrophage entry and phagocytosis after application of the ototoxin neomycin. We quantified macrophage entry and phagocytosis in response to neomycin treatment after pretreating larvae for 24 hr with 1, 10 or 50 µM dexamethasone Larvae that were not exposed to either neomycin and/or dexamethasone served as controls. All experiments followed the same protocol that we had previously used to characterize macrophage recruitment

320 and phagocytosis after neomycin toxicity (Warchol et al., 2021). Dexamethasone treatment did
321 not induce any significant changes to the subsequent macrophage response following neomycin
322 lesion (Fig. 5). Quantification revealed that the number of macrophage-hair cell contacts (Fig. 5
323 G) and number of phagocytotic events (Fig. 5 H) was similar in all neomycin treatment groups.
324 These observations indicate that pre- and co-treatment with 10 μM dexamethasone does not
325 suppress macrophage activation in response to neuromast injury.

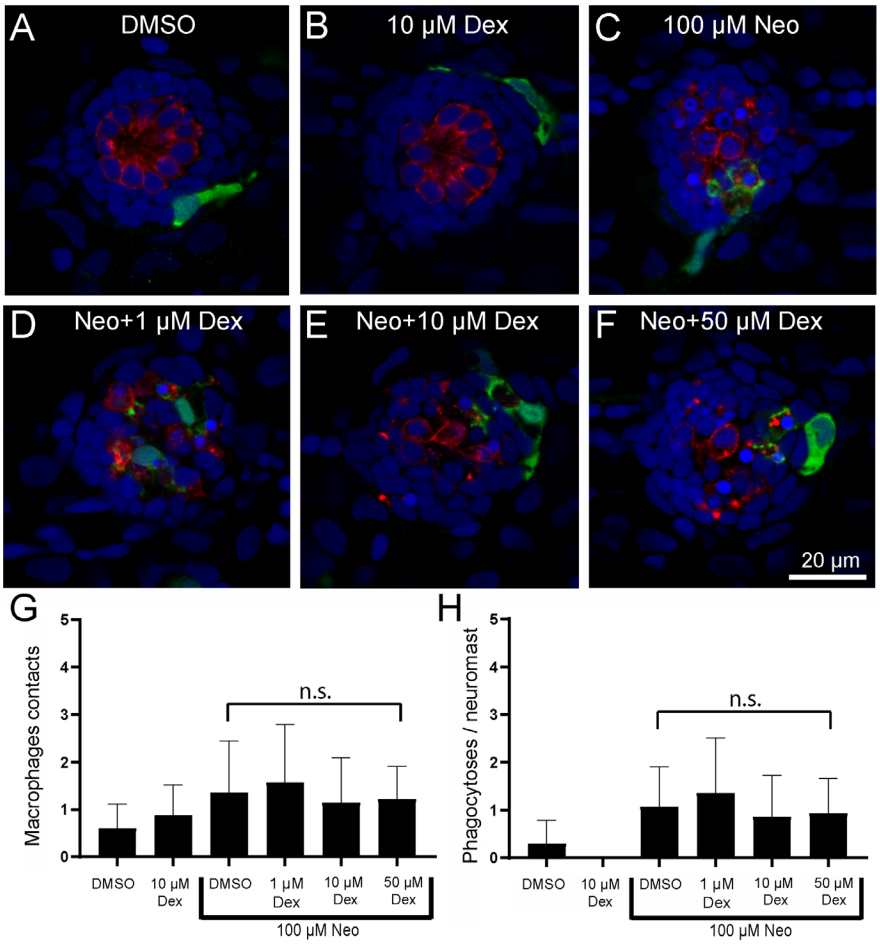

Figure 5. Dexamethasone did not inhibit macrophage response to neuromast injury
(A-F) Representative confocal images of control (A,B) and neomycin injured neuromasts (C-F). Larvae (6 dpf) were treated for 24 h with dexamethasone, then exposed for 30 min to neomycin. All specimens were fixed and processed for labeling of macrophages (green, YFP), hair cells (red, Otoferlin) and nuclei (blue, DAPI). Normal localization of macrophages was observed in control fish (A,B) and no inhibition was observed in neuromasts treated with neomycin (C-F). (G-H) Dexamethasone pretreatment did not affect macrophage contacts with dying hair cells (G, P>0.9999, Dunn's multiple comparison test) or the number of phagocytotic events (H, P>0.9999, Dunn's multiple comparison test). Bars indicate SD. N=15 fish/group; 2 experimental trials.

327 **Hair cell FM1-43 uptake and calcium homeostasis is unaffected by dexamethasone**
328 **exposure**

329 Numerous studies have indicated that dexamethasone can induce mitochondrial
330 dysfunction in various tissues, including adipocytes (Luan et al., 2019), skeletal muscle (Liu et
331 al., 2016), and neurons (Du et al., 2009). We previously reported reduced hair cell uptake of the
332 cationic dye FM1-43 in zebrafish mutants with impaired hair cell mitochondrial function (*mpv17*$^{-/-}$
333), indicating that these fish possessed reduced driving force for cations through
334 mechanotransduction channels, and elevated hair cell mitochondrial calcium (Holmgren &

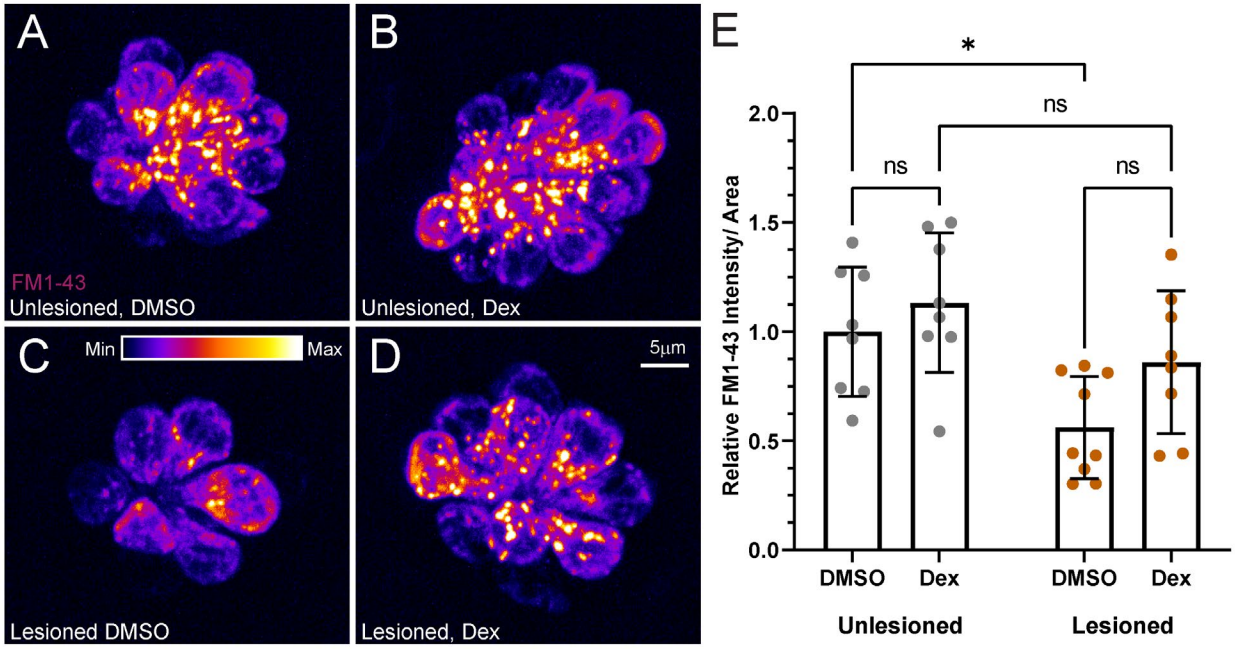

Figure 6. FM1-43 uptake was not significantly affected by dexamethasone exposure

(A-D) Representative maximum intensity projection images of pLL neuromasts in live 7dpf larvae immediately after brief (20 seconds) FM1-43 exposure. Neuromasts were either left intact (A, B) or lesioned with $CuSO_4$ (C, D), then allowed to regenerate for 48 hr while exposed to DMSO (carrier) (A, C) or dexamethasone (B, D) prior to FM1-43 exposure. The LUT bar (C) shows the range of intensity values, starting at 0 (min) to 400 (max). (E) Relative average FM1-43 intensity per neuromast. Scatter plots show raw integrated density (i.e. sum of the pixel values)/area values with SEM bars. Each dot represents the average values of neuromasts L3-L5 for one fish. Values were normalized for each experiment using the inverse median of the unlesioned control values. The data show no significant differences in intensity for dexamethasone-treated fish, relative to DMSO controls, in both intact and regenerating neuromasts (adjusted *P=0.0226). N=2-3 fish per condition per trial; 4 experimental trials.

Sheets, 2021). We therefore evaluated whether 48-hour dexamethasone exposure affected hair cell uptake of FM1-43 and calcium homeostasis. We observed no differences in FM1-43 uptake in unlesioned neuromasts that were treated in dexamethasone vs. those incubated in DMSO carrier (Fig. 6 A,B,E (gray circles)). In regenerating neuromasts, dexamethasone treatment appeared to cause a modest increase in FM1-43 uptake, but this trend did not reach statistical significance (Fig. 6 C-E (orange circles); adjusted P=0.1786). Notably, hair cells in regenerating DMSO-treated neuromasts (Fig. 6 C) displayed significantly reduced FM1-43 uptake relative to unlesioned DMSO-treated neuromasts (Fig. 6 A,E; adjusted *P=0.0226), indicating reduced mechanotransduction in regenerated control neuromast hair cells. By contrast, there was no significant difference in FM1-43 uptake in regenerating vs. unlesioned dexamethasone-treated neuromast hair cells (Fig. 6 B,D,E; adjusted P=0.2747), suggesting that dexamethasone treatment during regeneration may enhance hair cell regeneration and may also slightly impact the maturation of mechanotransduction.

We next examined hair cell cytosolic and mitochondrial calcium homeostasis using the genetically encoded calcium indicator GCaMP3 (Esterberg et al., 2013; Esterberg et al., 2014). When comparing unlesioned neuromasts and $CuSO_4$ lesioned neuromasts following regeneration, we observed average cytosolic calcium levels did not differ in neuromast hair cells (Fig. 7 A-E), while mitochondrial calcium levels appeared significantly higher in regenerating neuromast hair cells relative to unlesioned in both DMSO and dexamethasone treatment conditions (Fig. 7 F-J; adjusted ***P=0.0006 (DMSO), **P=0.0019 (Dex)). Notably, dexamethasone treatment had no effect on cytosolic or mitochondrial calcium levels relative to DMSO control in both unlesioned and regenerating neuromasts (Fig. 7 E, J). Cumulatively,

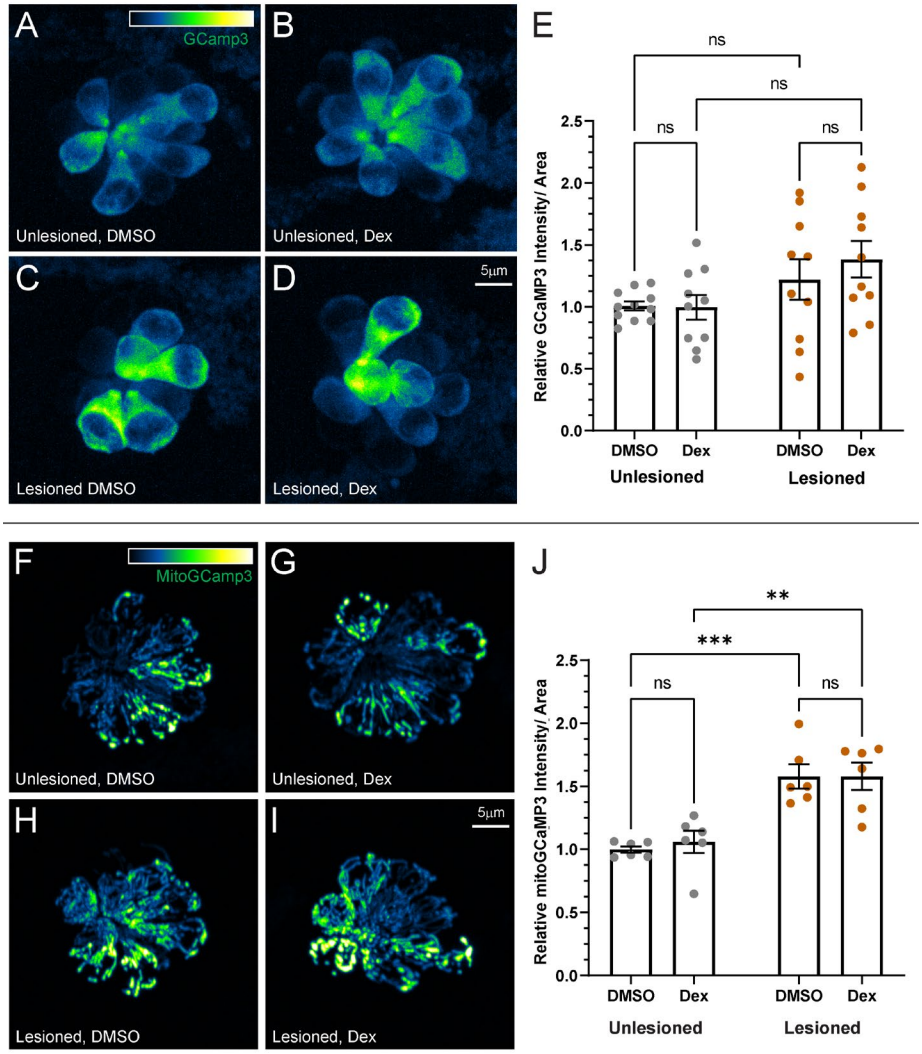

Figure 7. Dexamethasone did not affect hair cell cytosolic or mitochondrial calcium homeostasis

(A-D) Representative maximum intensity projection images of neuromasts in live 7dpf Tg(-6myo6b: GCaMP3) larvae. The LUT bar in (A) shows range of intensity values starting at 0 (min) to 2150 (max). (E) Hair cell GCaMP3 fluorescence intensity is not affected by dexamethasone exposure. Scatter plots of relative raw integrated intensity/area values with SEM bars. Each dot represents the average values of neuromasts L3-L5 for one fish. Data show no significant differences in intensity for dexamethasone-treated fish relative to DMSO controls in both intact and regenerating neuromasts. N=2-3 fish per condition per trial; 5 experimental trials (F-I) Representative images neuromasts in Tg(-6myo6b: mitoGCaMP3) larvae. LUT bar (F) shows range of intensity values starting at 0 (min) to 300 (max). (J) Hair cell mitoGCaMP fluorescence intensity is not affected by dexamethasone exposure but is elevated in regenerating neuromasts relative to intact neuromasts. Data show no significant differences in intensity for dexamethasone-treated fish relative to DMSO controls in both intact and regenerating neuromasts (adjusted ***P=0.0006 (DMSO), **P=0.0019 (Dex)). N=2-3 fish per condition per trial; 3 experimental trials.

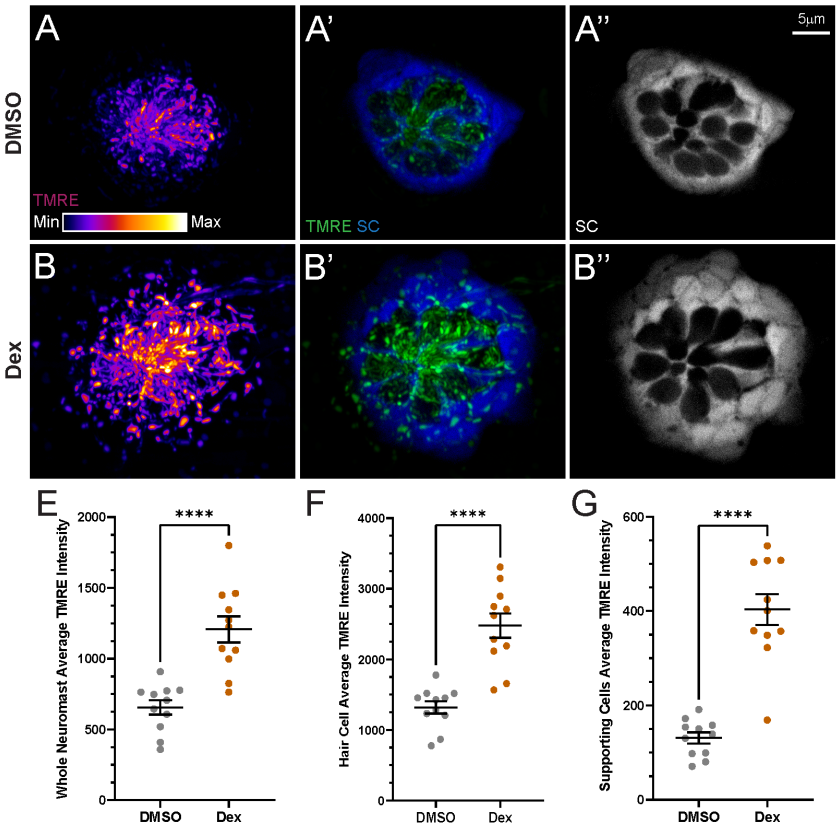

Figure 8. Dexamethasone exposure elevated mitochondrial activity in hair cells and supporting cells

(A-B) Confocal images of neuromasts in 7dpf fish following TMRE exposure. Fish were treated with DMSO (A) or dexamethasone (B) for 48 hours prior to imaging. TMRE (A, A', B, B') is shown as a max intensity projection and supporting cell (SC) images (A', A'', B', B'') are z-slices from the midlevel of the neuromast. Negative spaces inside GFP-labeled supporting cells indicate neuromast hair cells. LUT bar (A) shows range of intensity values starting at 0 (min) to 11800 (max). (E-G) Scatter plots of average TMRE fluorescence intensity with SEM bars. Dexamethasone-treated fish had significantly hyperpolarized mitochondria in both neuromast hair cells and supporting cells (adjusted **** P<0.0001). N=1-4 fish per condition per trial; 5 experimental trials.

these data suggest that prolonged dexamethasone exposure does not significantly impact hair cell mechanotransduction or affect calcium homeostasis in either intact or regenerating neuromasts.

Prolonged dexamethasone exposure hyperpolarizes neuromast mitochondria and sensitizes hair cells to neomycin

To determine whether 48-hour dexamethasone exposure impacted mitochondrial function in lateral-line neuromasts, we examined mitochondrial membrane potentials (ΔΨm) in unlesioned neuromast hair cells and supporting cells using tetramethylrhodamine methyl ester (TMRE)—a cell-permeant cationic dye used to assess mitochondrial function (Alassaf et al., 2019; Esterberg et al., 2016). Dexamethasone-exposed neuromasts had significantly higher TMRE mean fluorescence intensity relative to controls (Fig. 8 A,B,E; **** P<0.0001), indicating that mitochondria in dexamethasone-exposed neuromast cells are more hyperpolarized. Elevated TMRE fluorescence was apparent not only in the mitochondria of hair cells (Fig 8 A', B', F; EGFP-negative cells), but also the surrounding supporting cells (Fig 8 A", B", G; EGFP-positive cells), suggesting prolonged dexamethasone exposure disrupts normal mitochondrial function in both hair cells and supporting cells. Given that the hair cells in dexamethasone-

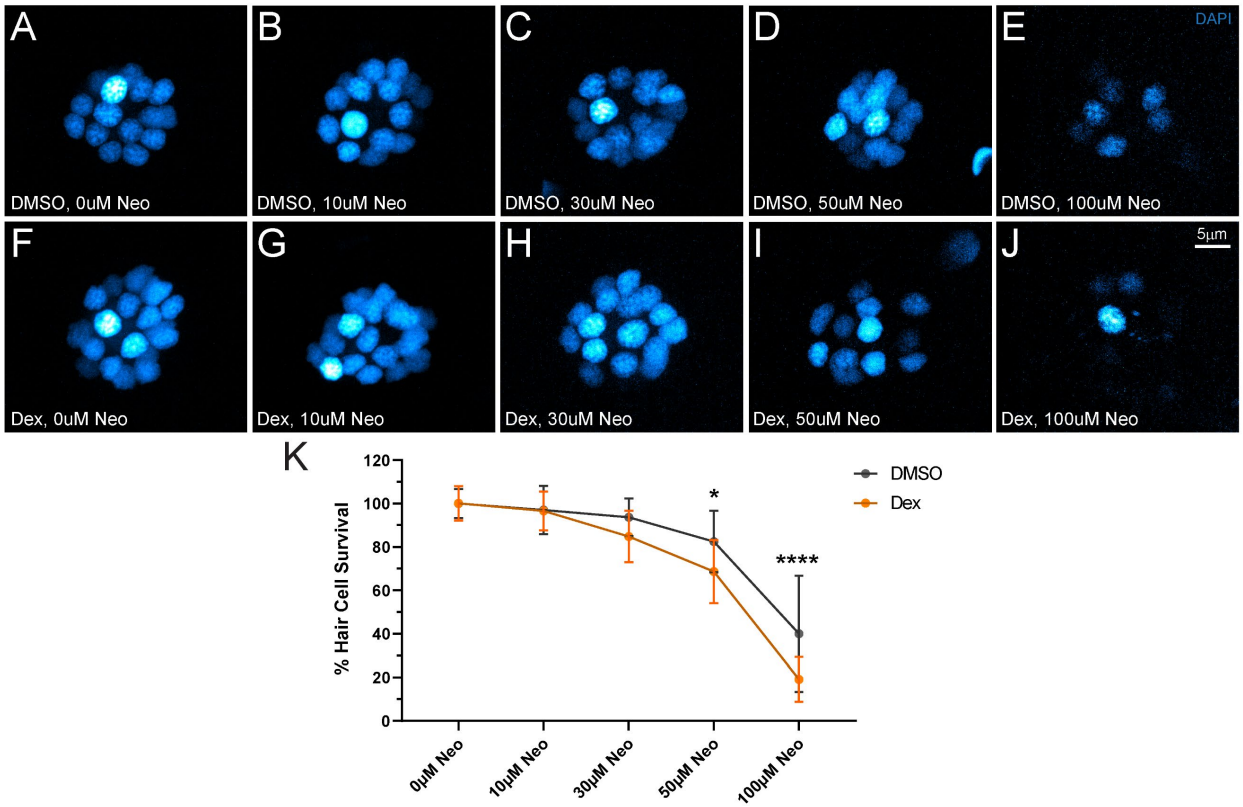

Figure 9. Dexamethasone exposure increased hair cell sensitivity to neomycin

(A-J) Representative maximum intensity images of DAPI-labeled neuromast hair cell nuclei (blue). Larvae (7dpf) were exposed for 48 hr to DMSO (carrier) alone (A-E) or dexamethasone (F-J), then exposed for 30min or 10µM (B, G), 30µM (C, H), 50µM (D, I), or 100µM (E, J) neomycin. EM buffer alone was used as a control (A,F). (K) Dose response curve with mean and SEM bars shows the number of surviving hair cells per neuromast as a percent of those present in unlesioned controls. Dexamethasone-treated neuromast hair cells were more sensitive to neomycin induced cell death than controls (adjusted P= 0.1407 (30 µM), *P=0.0353 (50 µM), ****P<0.0001 (100 µM)). N=7 fish per condition per trial; 3 experimental trials.

treated larvae had more negatively charged ΔΨm, we predicted that these hair cells would be more vulnerable to neomycin-induced hair cell death (Alassaf et al., 2019; Holmgren & Sheets, 2021). When treated with higher doses of neomycin (50-100 µM), we observed significantly more lateral-line hair cell loss in fish pre-exposed for 48 hours to dexamethasone, relative to controls (Fig 9 K; adjusted P= 0.1407 (30 µM), *P=0.0353 (50 µM), ****P<0.0001 (100 µM)). Thus, while prolonged dexamethasone does not appear to impact cytosolic or mitochondrial calcium homeostasis, it does alter neuromast mitochondrial function and increases hair cell sensitivity to neomycin-induced death.

Prolonged dexamethasone exposure reduces evoked calcium influx through mechanosensory hair bundles

Hair cells respond to sensory stimuli via deflection of apical hair bundles and opening of mechanotransduction channels. Influx of potassium and calcium occurs through these channels

410 which depolarizes the hair cell, leading to influx of calcium through basally-localized presynaptic
411 voltage-gated calcium channels, and triggering release of synaptic vesicles (Corey & Hudspeth,
412 1979; Moser & Beutner, 2000; Zhang et al., 2018). To determine if prolonged dexamethasone
413 exposure influenced hair cell responses to mechanical stimulation, we measured evoked
414 calcium influx at hair bundles and hair cell synapses in response to bundle deflection using a
415 transgenic line expressing plasma-membrane targeted GCaMP6s (Fig. 10 A;(Sheets et al.,
416 2017)). In response to a 500 ms step deflection, calcium influx at the hair bundle was

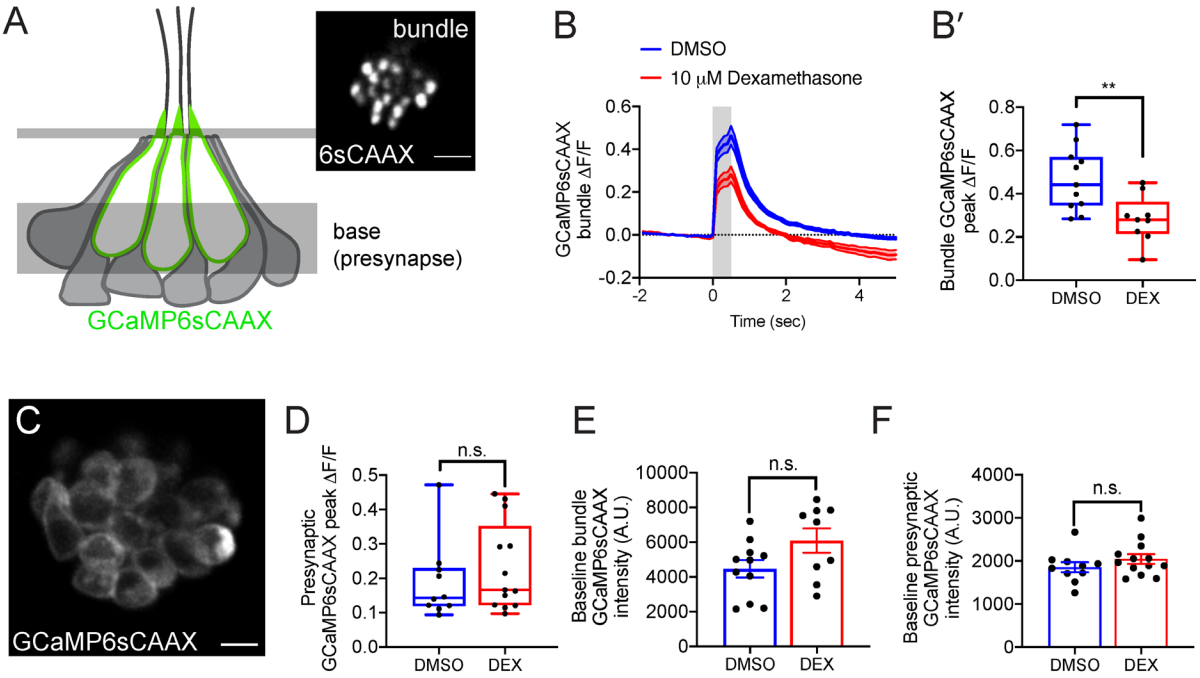

Figure 10. Dexamethasone exposure decreased evoked mechanosensation but not presynaptic calcium responses

(A) Schematic of a neuromast viewed from the side, and the imaging planes used to measure evoked calcium activity at the hair bundles and at the presynaptic region. Localization of GCaMP6sCAAX is shown in green. Inset shows an example of a top-down view of the hair bundle plane showing GCaMP6sCAAX fluorescence. (B-B') Evoked hair bundle calcium signal with (red) or without (blue) 48-hour dexamethasone pretreatment. Average traces are shown in B, while dot plots of peak response of bundles per neuromast are shown in B'. (C) Top-down view of the basal plane showing the presynaptic membrane labeled with GCaMP6sCAAX. (D) Dot plots show that the peak evoked presynaptic calcium signal averaged per neuromast with (red) and without (blue) 48-hour dexamethasone pretreatment. (E-F) Baseline calcium intensity with (red) and without (blue) dexamethasone treatment in hair bundles (E) and presynapses (F) Shaded area above and below traces in panel B and error bars in E-F represent SEM. Box-and-whiskers plot were used in B' and D to show median, min and max. An unpaired Welch's unequal variance *t*-test was used to calculate the significance of differences in B' and D. An unpaired *t*-test was used to calculate the significance of differences in E-F. n ≥ 9 neuromasts per treatment. **P=0.0052. Scale bar = 5 μm in A inset and C.

417 significantly reduced in dexamethasone-treated larvae relative to controls (Fig. 10 B,B'); an
418 unexpected result given that uptake of the cationic dye FM1-43 was not reduced in
419 dexamethasone-treated larvae (Fig. 5 A,B,E). By contrast, presynaptic calcium influx was not
420 significantly different in dexamethasone-treated fish vs. controls (Fig. 10 D). Baseline

421 GCaMP6sCAAX measurements at neuromast hair bundles and hair cell presynaptic regions
422 were comparable between dexamethasone-treated and control animals (Fig. 10 E,F), indicating
423 that calcium levels at rest were not altered in these two subcellular compartments. Overall,
424 these results provide evidence that prolonged dexamethasone exposure does not affect hair cell
425 calcium homeostasis but does negatively influence calcium flow through the hair bundle in
426 response to stimulus.

427 Discussion

428 Dexamethasone is a potent synthetic glucocorticoid that influences diverse molecular
429 pathways involved in cellular development, homeostasis, and repair. Using the zebrafish lateral
430 line as a model for hair cell organs, we examined the influence of prolonged dexamethasone
431 exposure on both afferent innervation of newly generated hair cells as well as hair cell
432 homeostasis and function. Following 48 hours of dexamethasone exposure, we observed no
433 inhibition of innervation or synapse formation in newly generated neuromast hair cells, indicating
434 that dexamethasone did not inhibit regeneration of afferent synaptic contacts in the lateral-line
435 system. However, further examination revealed prolonged dexamethasone exposure induced
436 mitochondrial hyperpolarization in neuromast hair cells and supporting cells, suggesting
437 disruption of mitochondrial homeostasis. In addition, dexamethasone exposure specifically
438 reduced evoked calcium influx at the hair bundle but not the hair cell synapse in response to
439 water-jet stimulus. Cumulatively, our data support that prolonged dexamethasone does not
440 inhibit newly generated hair cell innervation or synapse formation, but it may negatively impact
441 hair cell energy homeostasis and function.

442 **Dexamethasone did not inhibit lateral-line afferent nerve regrowth or hair cell synapse**
443 **formation during regeneration**

444 Exposure to dexamethasone significantly increased the total length of afferent neurites
445 per regenerating neuromast (Fig 3 C-E). The addition in nerve fiber length corresponds to the
446 increased number of hair cells (Fig. 3 F), suggesting that nerve fiber length was increased in
447 regenerating neuromasts to accommodate a larger number of newly formed hair cells.
448 Alternatively, it is possible that the additional neurites may be involved in facilitating hair cell
449 generation. A recent study characterizing functional lateral-line neuromast regeneration
450 following $CuSO_4$ ablation has reported that afferent nerve terminals formed initial contacts with
451 supporting cells during regeneration, suggesting that afferent nerve contacts may help facilitate
452 transdifferentiation of supporting cells into hair cells (Hardy et al., 2021). However, while
453 dexamethasone treatment caused regenerating neuromasts to add additional afferent dendrite

length, no such increase was observed in unlesioned neuromasts (Fig. 3 A,B,E), suggesting that the generation of additional hair cells in unlesioned neuromasts is not facilitated by additional nerve fiber contacts. Given that dexamethasone treatment did not increase the number of afferent synapses per hair cell in unlesioned neuromasts (Fig 4 E; gray circles), we posit that afferent neurons innervate and form synapses with newly generated hair cells in unlesioned larval neuromasts without adding additional processes.

We also did not observe inhibition of macrophage activation in response to ototoxic damage following dexamethasone pretreatment (Fig 5). This result provides additional support to a previously reported observation that dexamethasone likely enhances neuromast regeneration via a mechanism other than immunosuppression (Namdaran et al., 2012). Instead, dexamethasone may be acting though glucocorticoid receptors to enhance division of a subset of hair cell precursors. Further studies will be needed explore the cellular pathways underlying dexamethasone-induced hair cell generation, and the mechanistic differences between afferent nerve innervation and synapse formation in regenerating vs. intact neuromasts.

Prolonged dexamethasone exposure modulates mitochondrial membrane potential in neuromast cells and enhances neomycin hair cell toxicity

Glucocorticoid receptors reside in the cytosol of cells. When activated by a ligand such as cortisol or dexamethasone, they regulate gene expression by localizing to the cell nucleus and either directly binding to DNA or altering the activity of transcription factors or various kinases (Oakley & Cidlowski, 2013). Activated glucocorticoid receptors have also been shown to translocate into the mitochondria and regulate mitochondrial gene expression (Kokkinopoulou & Moutsatsou, 2021), and previous studies of mouse liver and rat distal colon have reported enhanced expression of mitochondrial genes involved in oxidative phosphorylation following dexamethasone treatment (Li et al., 2016; Rachamim et al., 1995). The glucocorticoid receptor gene *nr3c1* has been shown to be expressed in larval zebrafish neuromast hair cells and all populations of supporting cells (Lush et al., 2019). Speculatively, prolonged dexamethasone exposure may be modulating the expression of mitochondrial DNA encoded genes involved in oxidative phosphorylation, thereby altering mitochondrial metabolism in neuromast hair cells and supporting cells.

A recent study assessing the effects of cortisol exposure on hair cell sensitivity to neomycin further supports the hypothesis that activated glucocorticoid receptors regulates expression of genes that modulate mitochondrial metabolism (Hayward et al., 2019). Those authors reported that pretreatment of zebrafish larvae with cortisol for 24 hours sensitized neuromast hair cells to neomycin-induced hair cell death, which is comparable to what we

488 observed in dexamethasone-treated fish (Fig. 9). Cortisol-mediated sensitization to neomycin
489 was dependent on glucocorticoid receptor activation and could be blocked by inhibiting protein
490 translation. It is worth noting that Hayward et al. did not report a similar sensitization to
491 neomycin following 24 h dexamethasone exposure, but it is likely dexamethasone and cortisol
492 are acting through a shared mechanism. The difference between their reported observations
493 and our results is probably due to two factors. First, the concentration of neomycin used in
494 Hayward et al. following dexamethasone was 25 μM, which was two-fold less than the dose at
495 which we first observed significant effects ((Hayward et al., 2019); Fig 9 K). Also, the
496 dexamethasone pretreatment doses (0.001-1 μM vs. 10 μM) and exposure time (24 vs. 48
497 hours) used by Haywood et al., (2019) were less than those used in the present study.

498 **Prolonged dexamethasone exposure reduces evoked calcium influx though**
499 **mechanotransduction channels but does not affect hair cell calcium homeostasis**

500 While we did observe hyperpolarization of mitochondrial membrane potential in
501 dexamethasone-exposed neuromasts (Fig. 8), we did not observe significant changes in
502 cytosolic or mitochondrial calcium homeostasis within hair cells relative to controls (Fig 7). By
503 contrast, in response to water-jet stimuli, evoked calcium influx at the hair bundle was
504 significantly reduced (Fig. 10 B), suggesting calcium influx through activated MET channels is
505 reduced. This observed effect on calcium influx specifically at the hair bundle may be a
506 consequence of altered mitochondrial metabolism. Mitochondria are important regulators of
507 local intracellular calcium levels in sensory hair cells, and in addition to directly taking up
508 calcium, mitochondria provide ATP to drive clearance of calcium though plasma membrane
509 Ca^{2+}-ATPases (PMCA1 and PMCA2), with PMCA2 shown to be densely localized in the hair cell
510 stereocilia (Beurg et al., 2010). Zebrafish homologues of PMCA1 and PMCA2 are strongly
511 expressed in mature neuromast hair cells of larval zebrafish (Lush et al., 2019). It is possible
512 that altered mitochondrial metabolism may be influencing the activity of PMCA2 in
513 dexamethasone-treated hair cells, thereby modifying PMCA2 regulation of calcium levels at the
514 hair bundle. It is also conceivable that activated glucocorticoid receptors may be modulating
515 expression of genes involved in mechanotransduction channel calcium permeability. Further
516 experiments will be needed to determine the mechanism underlying dexamethasone's specific
517 effect on calcium influx through stimulated hair bundles.

518 In conclusion, our observations from zebrafish lateral-line neuromasts indicate that 48
519 hour dexamethasone treatment enhances regeneration and afferent reinnervation but alters
520 mitochondrial homeostasis and evoked calcium influx through hair bundles. Dexamethasone is
521 a steroid commonly used for treating hearing loss, and identifying strategies to retain high levels

522 of dexamethasone for long periods within the inner ear is currently an active area of research.
523 Considering our observations showing that prolonged exposure to dexamethasone had an
524 adverse effect on hair cell mitochondrial metabolism and impacted hair bundle calcium influx,
525 we believe future studies on the effects of long-term, localized dexamethasone treatment on
526 mammalian cochlear function are indicated.

527 Declaration of interests: The authors declare no competing financial or non-financial interests.

528 Acknowledgments: This work was supported by RIND (Grant ID G85; L.S.), a National Institute
529 on Deafness and Other Communication Disorders (NIDCD) Intramural Research Program Grant
530 1ZIADC000085-01 (K.S.K), and Extramural Research Project Grant R01DC006283 (M.E.W.).

531 References

532 Alassaf, M., Daykin, E. C., Mathiaparanam, J., & Wolman, M. A. (2019). Pregnancy-associated
533 plasma protein-aa supports hair cell survival by regulating mitochondrial function. *Elife*,
534 *8*. https://doi.org/10.7554/eLife.47061
535 Behra, M., Gallardo, V. E., Bradsher, J., Torrado, A., Elkahloun, A., Idol, J., Sheehy, J., Zonies,
536 S., Xu, L., Shaw, K. M., Satou, C., Higashijima, S., Weinstein, B. M., & Burgess, S. M.
537 (2012). Transcriptional signature of accessory cells in the lateral line, using the
538 Tnk1bp1:EGFP transgenic zebrafish line. *BMC Dev Biol*, *12*, 6.
539 https://doi.org/10.1186/1471-213X-12-6
540 Beurg, M., Nam, J. H., Chen, Q., & Fettiplace, R. (2010). Calcium balance and
541 mechanotransduction in rat cochlear hair cells. *J Neurophysiol*, *104*(1), 18-34.
542 https://doi.org/10.1152/jn.00019.2010
543 Bremer, J., Skinner, J., & Granato, M. (2017). A small molecule screen identifies in vivo
544 modulators of peripheral nerve regeneration in zebrafish. *PLoS One*, *12*(6), e0178854.
545 https://doi.org/10.1371/journal.pone.0178854
546 Corey, D. P., & Hudspeth, A. J. (1979). Ionic basis of the receptor potential in a vertebrate hair
547 cell. *Nature*, *281*(5733), 675-677. https://doi.org/10.1038/281675a0
548 Du, J., Wang, Y., Hunter, R., Wei, Y., Blumenthal, R., Falke, C., Khairova, R., Zhou, R., Yuan,
549 P., Machado-Vieira, R., McEwen, B. S., & Manji, H. K. (2009). Dynamic regulation of
550 mitochondrial function by glucocorticoids. *Proc Natl Acad Sci U S A*, *106*(9), 3543-3548.
551 https://doi.org/10.1073/pnas.0812671106
552 Egli Gallo, D., Khojasteh, E., Gloor, M., & Hegemann, S. C. (2013). Effectiveness of systemic
553 high-dose dexamethasone therapy for idiopathic sudden sensorineural hearing loss.
554 *Audiol Neurootol*, *18*(3), 161-170. https://doi.org/10.1159/000346938

555 Esterberg, R., Hailey, D. W., Coffin, A. B., Raible, D. W., & Rubel, E. W. (2013). Disruption of
556 intracellular calcium regulation is integral to aminoglycoside-induced hair cell death
557 [Research Support, N.I.H., Extramural]. *The Journal of neuroscience : the official journal*
558 *of the Society for Neuroscience*, *33*(17), 7513-7525.
559 https://doi.org/10.1523/JNEUROSCI.4559-12.2013
560 Esterberg, R., Hailey, D. W., Rubel, E. W., & Raible, D. W. (2014). ER-mitochondrial calcium
561 flow underlies vulnerability of mechanosensory hair cells to damage [Research Support,
562 N.I.H., Extramural]. *The Journal of neuroscience : the official journal of the Society for*
563 *Neuroscience*, *34*(29), 9703-9719. https://doi.org/10.1523/JNEUROSCI.0281-14.2014
564 Esterberg, R., Linbo, T., Pickett, S. B., Wu, P., Ou, H. C., Rubel, E. W., & Raible, D. W. (2016).
565 Mitochondrial calcium uptake underlies ROS generation during aminoglycoside-induced
566 hair cell death. *J Clin Invest*, *126*(9), 3556-3566. https://doi.org/10.1172/JCI84939
567 Feng, X., & Yuan, W. (2015). Dexamethasone enhanced functional recovery after sciatic nerve
568 crush injury in rats. *Biomed Res Int*, *2015*, 627923. https://doi.org/10.1155/2015/627923
569 Fernandez, R., Harrop-Jones, A., Wang, X., Dellamary, L., LeBel, C., & Piu, F. (2016). The
570 Sustained-Exposure Dexamethasone Formulation OTO-104 Offers Effective Protection
571 against Cisplatin-Induced Hearing Loss. *Audiol Neurootol*, *21*(1), 22-29.
572 https://doi.org/10.1159/000441833
573 Ge, H., Ni, S., Wang, X., Xu, N., Liu, Y., Wang, X., Wang, L., Song, D., Song, Y., & Bai, C.
574 (2012). Dexamethasone reduces sensitivity to cisplatin by blunting p53-dependent
575 cellular senescence in non-small cell lung cancer. *PLoS One*, *7*(12), e51821.
576 https://doi.org/10.1371/journal.pone.0051821
577 Hardy, K., Amariutei, A. E., De Faveri, F., Hendry, A., Marcotti, W., & Ceriani, F. (2021).
578 Functional development and regeneration of hair cells in the zebrafish lateral line. *J*
579 *Physiol*, *599*(16), 3913-3936. https://doi.org/10.1113/JP281522
580 Hayward, T., Young, A., Jiang, A., Crespi, E. J., & Coffin, A. B. (2019). Glucococorticoid
581 receptor activation exacerbates aminoglycoside-induced damage to the zebrafish lateral
582 line. *Hear Res*, *377*, 12-23. https://doi.org/10.1016/j.heares.2019.03.002
583 Holmgren, M., & Sheets, L. (2021). Influence of Mpv17 on Hair-Cell Mitochondrial Homeostasis,
584 Synapse Integrity, and Vulnerability to Damage in the Zebrafish Lateral Line. *Front Cell*
585 *Neurosci*, *15*, 693375. https://doi.org/10.3389/fncel.2021.693375
586 Kokkinopoulou, I., & Moutsatsou, P. (2021). Mitochondrial Glucocorticoid Receptors and Their
587 Actions. *Int J Mol Sci*, *22*(11). https://doi.org/10.3390/ijms22116054

588 Li, R., Jia, Y., Pan, S., Li, X., Song, H., & Zhao, R. (2016). Glucocorticoid Receptor Mediates the
589 Effect of High-Fat Diet on Mitochondrial Oxidative Phosphorylation in Mouse Liver. *DNA*
590 *Cell Biol*, *35*(2), 51-58. https://doi.org/10.1089/dna.2015.2932
591 Liao, A. H., Shih, C. P., Li, M. W., Lin, Y. C., Chuang, H. C., & Wang, C. H. (2021).
592 Development of thermosensitive poloxamer 407-based microbubble gel with ultrasound
593 mediation for inner ear drug delivery. *Drug Deliv*, *28*(1), 1256-1271.
594 https://doi.org/10.1080/10717544.2021.1938758
595 Liu, J., Peng, Y., Wang, X., Fan, Y., Qin, C., Shi, L., Tang, Y., Cao, K., Li, H., Long, J., & Liu, J.
596 (2016). Mitochondrial Dysfunction Launches Dexamethasone-Induced Skeletal Muscle
597 Atrophy via AMPK/FOXO3 Signaling. *Mol Pharm*, *13*(1), 73-84.
598 https://doi.org/10.1021/acs.molpharmaceut.5b00516
599 Longair, M. H., Baker, D. A., & Armstrong, J. D. (2011). Simple Neurite Tracer: open source
600 software for reconstruction, visualization and analysis of neuronal processes.
601 *Bioinformatics*, *27*(17), 2453-2454. https://doi.org/10.1093/bioinformatics/btr390
602 Luan, G., Li, G., Ma, X., Jin, Y., Hu, N., Li, J., Wang, Z., & Wang, H. (2019). Dexamethasone-
603 Induced Mitochondrial Dysfunction and Insulin Resistance-Study in 3T3-L1 Adipocytes
604 and Mitochondria Isolated from Mouse Liver. *Molecules*, *24*(10).
605 https://doi.org/10.3390/molecules24101982
606 Lukasz, D., & Kindt, K. S. (2018). In Vivo Calcium Imaging of Lateral-line Hair Cells in Larval
607 Zebrafish. *J Vis Exp*(141). https://doi.org/10.3791/58794
608 Lush, M. E., Diaz, D. C., Koenecke, N., Baek, S., Boldt, H., St Peter, M. K., Gaitan-Escudero,
609 T., Romero-Carvajal, A., Busch-Nentwich, E. M., Perera, A. G., Hall, K. E., Peak, A.,
610 Haug, J. S., & Piotrowski, T. (2019). scRNA-Seq reveals distinct stem cell populations
611 that drive hair cell regeneration after loss of Fgf and Notch signaling. *Elife*, *8*.
612 https://doi.org/10.7554/eLife.44431
613 Mackenzie, S. M., & Raible, D. W. (2012). Proliferative regeneration of zebrafish lateral line hair
614 cells after different ototoxic insults [Research Support, N.I.H., Extramural]. *PLoS One*,
615 *7*(10), e47257. https://doi.org/10.1371/journal.pone.0047257
616 Marshak, T., Steiner, M., Kaminer, M., Levy, L., & Shupak, A. (2014). Prevention of Cisplatin-
617 Induced Hearing Loss by Intratympanic Dexamethasone: A Randomized Controlled
618 Study. *Otolaryngol Head Neck Surg*, *150*(6), 983-990.
619 https://doi.org/10.1177/0194599814524894
620 Michanski, S., Smaluch, K., Steyer, A. M., Chakrabarti, R., Setz, C., Oestreicher, D., Fischer,
621 C., Mobius, W., Moser, T., Vogl, C., & Wichmann, C. (2019). Mapping developmental

622 maturation of inner hair cell ribbon synapses in the apical mouse cochlea. *Proc Natl*
623 *Acad Sci U S A*, *116*(13), 6415-6424. https://doi.org/10.1073/pnas.1812029116
624 Moser, T., & Beutner, D. (2000). Kinetics of exocytosis and endocytosis at the cochlear inner
625 hair cell afferent synapse of the mouse. *Proc Natl Acad Sci U S A*, *97*(2), 883-888.
626 https://doi.org/10.1073/pnas.97.2.883
627 Namdaran, P., Reinhart, K. E., Owens, K. N., Raible, D. W., & Rubel, E. W. (2012).
628 Identification of modulators of hair cell regeneration in the zebrafish lateral line
629 [Comparative Study
630 Research Support, N.I.H., Extramural]. *The Journal of neuroscience : the official journal of the*
631 *Society for Neuroscience*, *32*(10), 3516-3528.
632 https://doi.org/10.1523/JNEUROSCI.3905-11.2012
633 Oakley, R. H., & Cidlowski, J. A. (2013). The biology of the glucocorticoid receptor: new
634 signaling mechanisms in health and disease. *J Allergy Clin Immunol*, *132*(5), 1033-1044.
635 https://doi.org/10.1016/j.jaci.2013.09.007
636 Obholzer, N., Wolfson, S., Trapani, J. G., Mo, W., Nechiporuk, A., Busch-Nentwich, E., Seiler,
637 C., Sidi, S., Sollner, C., Duncan, R. N., Boehland, A., & Nicolson, T. (2008). Vesicular
638 glutamate transporter 3 is required for synaptic transmission in zebrafish hair cells
639 [Research Support, N.I.H., Extramural]. *The Journal of neuroscience : the official journal*
640 *of the Society for Neuroscience*, *28*(9), 2110-2118.
641 https://doi.org/10.1523/JNEUROSCI.5230-07.2008
642 Ohnmacht, J., Yang, Y., Maurer, G. W., Barreiro-Iglesias, A., Tsarouchas, T. M., Wehner, D.,
643 Sieger, D., Becker, C. G., & Becker, T. (2016). Spinal motor neurons are regenerated
644 after mechanical lesion and genetic ablation in larval zebrafish. *Development*, *143*(9),
645 1464-1474. https://doi.org/10.1242/dev.129155
646 Olivari, F. A., Hernandez, P. P., & Allende, M. L. (2008). Acute copper exposure induces
647 oxidative stress and cell death in lateral line hair cells of zebrafish larvae. *Brain Res*,
648 *1244*, 1-12. https://doi.org/10.1016/j.brainres.2008.09.050
649 Patel, M. (2017). Intratympanic corticosteroids in Meniere's disease: A mini-review. *J Otol*,
650 *12*(3), 117-124. https://doi.org/10.1016/j.joto.2017.06.002
651 Rachamim, N., Latter, H., Malinin, N., Asher, C., Wald, H., & Garty, H. (1995). Dexamethasone
652 enhances expression of mitochondrial oxidative phosphorylation genes in rat distal
653 colon. *Am J Physiol*, *269*(5 Pt 1), C1305-1310.
654 https://doi.org/10.1152/ajpcell.1995.269.5.C1305

655 Roca, F. J., & Ramakrishnan, L. (2013). TNF dually mediates resistance and susceptibility to
656 mycobacteria via mitochondrial reactive oxygen species. *Cell*, *153*(3), 521-534.
657 https://doi.org/10.1016/j.cell.2013.03.022
658 Salt, A. N., Hartsock, J., Plontke, S., LeBel, C., & Piu, F. (2011). Distribution of dexamethasone
659 and preservation of inner ear function following intratympanic delivery of a gel-based
660 formulation. *Audiol Neurootol*, *16*(5), 323-335. https://doi.org/10.1159/000322504
661 Schneider, C. A., Rasband, W. S., & Eliceiri, K. W. (2012). NIH Image to ImageJ: 25 years of
662 image analysis. *Nat Methods*, *9*(7), 671-675. https://doi.org/10.1038/nmeth.2089
663 Sheets, L., He, X. J., Olt, J., Schreck, M., Petralia, R. S., Wang, Y. X., Zhang, Q., Beirl, A.,
664 Nicolson, T., Marcotti, W., Trapani, J. G., & Kindt, K. S. (2017). Enlargement of Ribbons
665 in Zebrafish Hair Cells Increases Calcium Currents But Disrupts Afferent Spontaneous
666 Activity and Timing of Stimulus Onset. *J Neurosci*, *37*(26), 6299-6313.
667 https://doi.org/10.1523/JNEUROSCI.2878-16.2017
668 Suli, A., Pujol, R., Cunningham, D. E., Hailey, D. W., Prendergast, A., Rubel, E. W., & Raible, D.
669 W. (2016). Innervation regulates synaptic ribbons in lateral line mechanosensory hair
670 cells. *Development*, *143*(12), e1 2. https://doi.org/10.1242/dev.140616
671 Valledor, A. F., & Ricote, M. (2004). Nuclear receptor signaling in macrophages. *Biochem*
672 *Pharmacol*, *67*(2), 201-212. https://doi.org/10.1016/j.bcp.2003.10.016
673 Vettorazzi, S., Nalbantoglu, D., Gebhardt, J. C. M., & Tuckermann, J. (2021). A guide to
674 changing paradigms of glucocorticoid receptor function-a model system for genome
675 regulation and physiology. *FEBS J*. https://doi.org/10.1111/febs.16100
676 Waissbluth, S., Salehi, P., He, X., & Daniel, S. J. (2013). Systemic dexamethasone for the
677 prevention of cisplatin-induced ototoxicity. *Eur Arch Otorhinolaryngol*, *270*(5), 1597-
678 1605. https://doi.org/10.1007/s00405-012-2150-0
679 Warchol, M. E., Schrader, A., & Sheets, L. (2021). Macrophages Respond Rapidly to Ototoxic
680 Injury of Lateral Line Hair Cells but Are Not Required for Hair Cell Regeneration. *Front*
681 *Cell Neurosci*, *14*, 613246. https://doi.org/10.3389/fncel.2020.613246
682 Zhang, Q., Li, S., Wong, H. C., He, X. J., Beirl, A., Petralia, R. S., Wang, Y. X., & Kindt, K. S.
683 (2018). Synaptically silent sensory hair cells in zebrafish are recruited after damage. *Nat*
684 *Commun*, *9*(1), 1388. https://doi.org/10.1038/s41467-018-03806-8

685